Atomization of two colliding micro liquid jets in a respiratory inhaler: A computational study

Mahdi Saeedipour*[1]
[1]Department of Particulate Flow Modelling, Johannes Kepler University, A-4040 Linz, Austria
*Corresponding author: mahdi.saeedipour@jku.at

Abstract
Inhaling respiratory drugs is a widespread method to treat a variety of pulmonary diseases. The efficacy of these medications is strongly dependent on the spray cloud characteristics generated by the inhaler device. In the present study, we investigate the atomization of the liquid drug into small inhalable droplets out of a soft mist inhaler. In this device, the drug solution is forced through two converging nozzle channels to generate two laminar micro liquid jets which collide obliquely in the downstream of the nozzles and form a spray cloud. Because of the nozzles' microscopic dimensions and high pressure provided by the device, the jets collide under a high Weber number condition and form a wavy sheet that remains in a so-called impact wave regime. This leads to disintegration of ligaments from the leading edge of the sheet and their further breakup into small droplets. An open-source, geometrical volume of fluid model (VOF) is employed to simulate the jets collision and track the liquid-gas interfaces from the sheet down to the small droplets. A post-processing tool based on connected-component labelling concept is developed to detect the resolved droplets and obtain the droplet sizes. Different design parameters such as the jets velocity, shape, and collision angle as well as the drug solution surface tension were varied to investigate different cases. The impinged sheet properties such frequency of impact waves as well as the cloud properties such as characteristic mean diameter are computed and used as comparison measures between the cases. The simulation results demonstrate that increasing the injection velocities as well as decreasing the surface tension increases the instability of impact waves and the sheet lateral motion which enhances the atomization. Also, the collision angle is found proportional to the backward liquid flow from the sheet region. In addition, the jets cross-section shape is found an essential parameter to control the circumferential dispersion of the droplets for the future design of small inhalers.

Keywords
Colliding atomization, medical spray, volume of fluid method (VOF), microfluidics, CFD

Introduction

Respiratory drug delivery is a widespread treatment method for many pulmonary diseases. It is an advantageous alternative to the oral rout due to less required drug dosage and minimized side effects. For this purpose, the aqueous drug solution has to be disintegrated into microscopic inhalable aerosol droplets by the inhaler device. The size of these droplets has to be fine enough to penetrate into the lungs. The complex physics of the drug spray generation, sustainable mechanical production and the significance of medical factors such as dosage control and patient compliance have made the design and manufacturing of inhaler devices a multidisciplinary area of research. Currently, there are three categories of inhalers [1]: (i) pressurized metered dose inhalers (pMDI) in which the drug solution is formulated under pressure of a liquid propellant, (ii) dry powder inhalers (DPI) in which the stored drug powder is delivered by the act of breathing and (iii) nebulizers in which the drug solution is atomized into small droplets through different mechanisms. Among the novel designs of nebulizers, the *Respimat*® soft mist inhaler (SMI) has shown a relatively good performance in generating fine aerosol droplets with a relatively slow spray front propagation compared to pMDI. Being portable, easy-to-use and propellant-free, this inhaler device has attracted a considerable attention in the past years [4]. In this device, the drug solution is forced through two converging micro-channels typically on the order of 10 microns [3] generate two laminar micro liquid jets which then collide obliquely in the downstream of the nozzles and form a spray cloud. Because of the nozzles' microscopic dimensions and the relatively high pressure gradient (i.e. hundreds of atmospheres [1]), the jets collide under a high Weber number (We) condition and form a wavy sheet that remains in a so-called impact wave regime [2]. This leads to disintegration of ligaments from the leading edge of the sheet and their further breakup into small droplets in the order of few microns. The required mechanical energy is supplied by a spring-driven piston [3] activated by turning the inhaler base by the patient [4].

The physics of two liquid jets impingement and the consequent colliding atomization have been studied extensively [5-8]. By experiments [9] and according to the dimensionless numbers of Reynolds (Re) and Weber, various

colliding atomization regimes have been identified. These regimes are sorted as liquid chain (low Re and We), closed and open rims (moderate Re and We) and turbulent impact wave (high Re and We) [9-10]. In the latter case, the loss of energy at the jets impingement point causes an instability that entails the fluctuation of the sheet with a certain fundamental frequency [5, 11]. These generated waves play the major role in atomization for this regime. It has to be noted that some theoretical models have been proposed for the characteristics of the impinged sheet and the size of droplets in the literature [12]. But, since the SMI device always operates under the impact wave regime, these models are not discussed in this paper. A recent literature review can be found in [13].
From the multiphase flow modelling aspect, the most typical approach to simulate the colliding atomization is the Eulerian one-fluid formulation where the Navier-Stokes equations with one shared velocity field between two-phases are coupled with an interface capturing techniques such as volume of fluid method (VOF) [14]. Examples include the studies conducted by Chen et al. [10], Zhang and Wang [11], and Ruan et al, [15] in which they employed the geometrical VOF with adaptive mesh refinement (AMR) using *Gerris* code [16]. They studied the flow characteristics and the statistics of produced sprays at different operating conditions in agreement with corresponding experimental investigations. Using the algebraic VOF with AMR in OpenFOAM [17], Dolatkhahi et al., studied the atomization pattern of two similar and dissimilar liquid jets at different conditions [18].

Despite the extensive previous studies on colliding atomization, the micro-scale physical dimensions of the nozzles in the portable inhalers on the one hand, and the active state of patent and marketing [3], on the other hand have led to a rather scarce literature on the spray formation in such small devices. To the author's best knowledge, the colliding atomization in the SMI has not been explored analytically or numerically. Besides, no detailed knowledge on the microfluidic nozzles' shapes, upstream nozzle structure as well as the characteristics of the downstream flow has been published. Using computational fluid dynamics (CFD), the present study attempts to investigate the physics of colliding atomization of two microfluidic jets in the soft mist inhaler. A recently-developed OpenFOAM-based VOF method called *isoAdvector* [19] is employed to perform the numerical simulation. Different design parameters such as the jets velocity, shape, and collision angle as well as the drug solution surface tension were varied to investigate different conditions. The sheet properties such as frequency of impact waves as well as the cloud properties such as characteristic mean diameter of D_{90} are computed and used as comparison measures between the cases. This study provides a first systematic evaluation on the colliding atomization of soft mist inhaler for the future design of small inhalers.

Description of the respiratory inhaler

The Respimat® soft mist inhaler is a pocket-sized device as shown in Figure 1-(a). It is used to generate a cloud of very fine aerosol droplets (i.e. < 5 μm) with sufficiently slow front propagation and independent of the patient's inspiration. It is manufactured by Boehringer Ingelheim company and is currently used for different lung diseases.

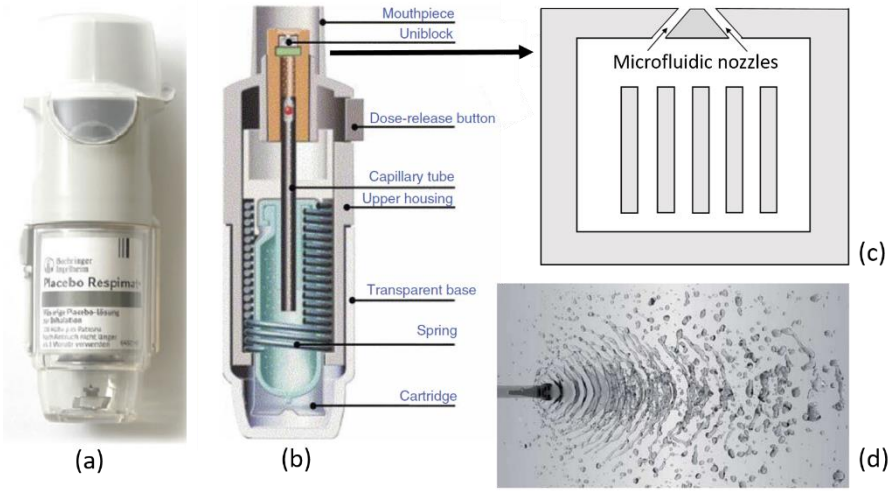

Figure 1. (a) The latest design of Respimat® soft mist inhaler [4], (b) the schematic of internal structure of the device [1], (c) schematic of the Uniblock component with the microfluidic nozzles at the top (redrawn from [3]), and (d) flow representation of impact wave atomization regime [10].

The colliding atomization occurs at the top of the device where the microfluidic nozzles are placed. According to [2], the key component responsible for spray formation is placed at the top of device and called the Uniblock. The Uniblock comprises two microfluidic nozzle outlets of small dimensions (i.e. 5.6 x 8 μm) [2]. To prevent the nozzles

from clogging, it has a particular design which is depicted in Figure 1-(c) schematically. By twisting the base of the device and upon actuation, a pressure up to 250 bar [2] pushes the drug solution through the nozzles which form two oblique micro liquid jets with the average velocity of 112 m/s for the duration of 1.5 s. The exact collision angle has not been reported, but according to [20] it is approximately 90 degrees. These small jets collide with Re= 738 and We= 1840 and form a sheet which is typically in the impact wave regime. A numerical representation of this colliding atomization regime is reprinted from [10] in Figure 1-(d).

Numerical method description

The governing equations for an incompressible, immiscible liquid-gas flow within the one-fluid formulation are the continuity and Navier–Stokes equations together with the advection equation of volume of fluid as follows:

$$\frac{\partial \rho}{\partial t} + \nabla \cdot (\rho \boldsymbol{U}) = 0 \tag{1}$$

$$\frac{\partial (\rho \boldsymbol{U})}{\partial t} + \nabla \cdot (\rho \boldsymbol{U} \otimes \boldsymbol{U}) = -\nabla p + \nabla \cdot (2\mu \boldsymbol{D}) + \rho \boldsymbol{g} + \boldsymbol{S}_\sigma \tag{2}$$

$$\frac{\partial \alpha}{\partial t} + \nabla \cdot (\alpha \boldsymbol{U}) = 0 \tag{3}$$

In this formulation, $\boldsymbol{U}$ is the mixture velocity vector shared with both phases, p is the pressure and $\boldsymbol{D}$ is the rate of deformation tensor. The scalar α is the volume fraction which determines the physical properties of the flow in one-fluid assumption based on the liquid and gas material properties: $\rho = \alpha\rho_l + (1-\alpha)\rho_g$ and $\mu = \alpha\mu_l + (1-\alpha)\mu_g$. The surface tension force is computed at the interface region by the Continuous Surface Force method (CSF) [21] and reads

$$\boldsymbol{S}_\sigma = \sigma \kappa \hat{n} \delta_s \tag{4}$$

Here, the interface normal vector $\hat{n}$ and curvature κ are usually approximated by the first and second derivatives of volume fraction as:

$$\hat{n} = \frac{\nabla \alpha}{|\nabla \alpha|} \tag{5}$$

$$\kappa = -\nabla \cdot \hat{n} = -\nabla \cdot \left(\frac{\nabla \alpha}{|\nabla \alpha|}\right) \tag{6}$$

However, this estimation is a challenging task due to the discontinuous nature of α. In the VOF approach, two major steps need to be handled for accurate interface capturing: (i) advection of phase indicator function, and (ii) estimation of interface curvature. There are two families of advection methodologies: geometrical and algebraic. Geometrical methods are based on explicit reconstruction of interface from volume fraction field. In return, algebraic methods do not involve the geometrical reconstruction but they preserve sharp interface by adding an artificial compression term to the VOF equation. This makes algebraic VOF faster and easier to implement. A well-known example of algebraic VOF is the Multidimensional Universal Limiter of Explicit Solution (MULES) algorithm available in OpenFOAM. However, algebraic VOF suffers from lack of accuracy compared to geometrical VOF, in particular for the flows where the small-scale interfacial structures are intended to be pictured. To circumvent this limitation and yet keep the minimum geometrical consideration, Roenby et al. [19] have developed a geometrical VOF in the framework of OpenFOAM called *isoAdvector*. They replaced the MULES algorithm with a two-step reconstruction/propagation operation based on iso-surface of volume fraction in each computational cell. Their approach demonstrates a satisfactory results for 2D and 3D benchmark problems, where the algebraic VOF performs poorly [19]. Therefore in this study, the isoAdvector method is employed for the VOF simulation of the micro liquid jets collisions, impinged sheet dynamics and the downstream spray formation.

Post-processing tool for spray properties

One of the challenging task in numerical modelling of atomization using interface capturing methods is to extract the spray properties statistics of CFD simulation data. In this study, we developed a post-processing tool inspired from the connected-component labelling concept to identify the coherent liquid structures and calculate their sizes. This method is analogous to the algorithm presented in Vallier et al. [22] for detecting dispersed bubbles in the computational domain and replacing them with tracer massless particles within an Eulerian-Lagrangian simulation.

First, the computational cells with $\alpha > \alpha_{tr}$ are selected. The α_{tr} is a threshold value which is chosen 0.25 in this study. These are the potential cells for containing coherent liquid structures. By means of the hash-table functionality in OpenFOAM, each cell (key) receives a droplet ID (value). By making loops over the keys and their adjacent cells, and updating the hash-table, a series of connected cells with similar value (i.e. droplet ID) is identified as schemed in Figure 2-(a). The liquid volume in each group reads $V_{ID} = \sum_{i \in ID} \alpha_i V_i$. An equivalent spherical droplet is assigned to each group (Figure 2-(b)). These droplets can be used for size distribution and statistical analysis. This algorithm is programmed within the C++ libraries of OpenFOAM and can be used for 2D and 3D simulations.

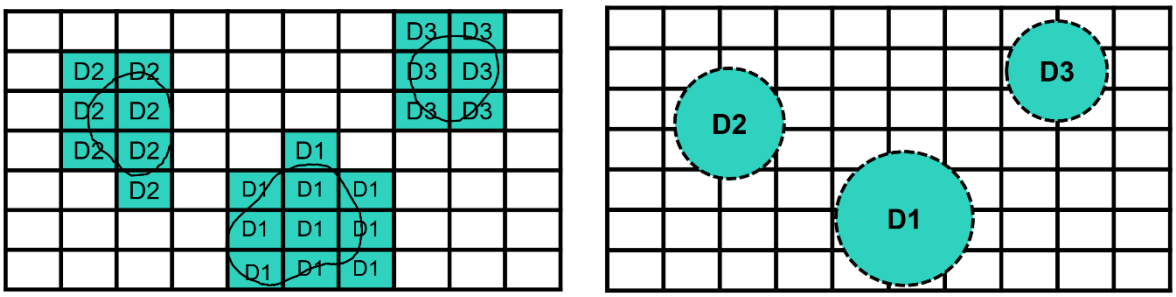

Figure 2. Schematic discerption of post-processing tool: (a) the connected cells identification with the same ID, and (b) the equivalent droplet assigned to each connected structure.

Simulation setup

To investigate the atomization of two colliding microfluidic jets, the SMI device at its reported operating conditions [2] is selected as the reference case (hereinafter C-1). By varying the operating parameters such as the jets velocity, shape, and collision angle as well as the drug solution surface tension, seven more cases are considered as all presented in Table 1.

Table 1. The operating parameters for the different simulation cases.

case	C-1	C-2	C-3	C-4	C-5	C-6	C-7	C-8
U (m/s)	112	112	90	135	112	112	112	112
2θ (°)	90	90	90	90	90	90	60	120
σ (N/m)	0.044	0.044	0.044	0.044	0.072	0.016	0.044	0.044
jet shape	Plain	Round	Plain	Plain	Plain	Plain	Plain	Plain

A three-dimensional geometry (L_x = 80 µm, L_y = 400 µm and L_z = 100 µm) with two rectangular inlets at the left patch (5.6 x 8 µm) was created as the computational domain (depicted in Figure 3). For the case of round inlets (i.e. C-2) the hydraulic diameter of D_h = 6 µm is applied. The inlet velocity corresponding to the injection angles and zero gradient outlet boundary conditions were imposed at the inlets and surrounding open boundaries, respectively. A no-slip boundary condition is considered for the velocity at the patch around the inlets. The domain was discretized uniformly with the grid size of 2 µm, followed by refinement for the inlet regions (Δx = 0.5 µm) and the middle one-fifth of L_x (Δx = 1 µm). This resulted in almost 1,800,000 total computational cells. The Navier-Stokes equations were solved together with the VOF equation utilizing the solver package of *interflow* which is the OpenFOAM-based solver including the isoAdvector method. The PIMPLE algorithm is adopted for pressure-velocity coupling and pressure correction. In this study, large eddy simulation (LES) is accounted for turbulence treatment in which a classic eddy viscosity-based model is employed to close the convective subgrid term. A first-order implicit discretization scheme is used for the temporal term. A second-order Gaussian discretization scheme is used for the convective and gradient terms. Also, the Van Leer scheme [17] is used for the discretization of the convective term in the VOF. The simulation time steps were adjusted during the simulation based on CFL criterion to keep the maximum Courant number of 0.5 and the maximum interface Courant number of 0.2. The simulations were performed until a quasi-steady state condition was achieved for the size distribution of the droplets (i.e. D_{90}). Thus, a duration of 100 µs was simulated for each case using 24 processors on an in-house computational cluster.

Results and discussions

The global structure of the spray developed from the colliding atomization as well as a top view of the impinged sheet for the C-1 are illustrated in Figure 4. The snapshots are taken after the 100 µs when the spray has reached a steady-state condition. The cumulative size distribution of the droplets after 100 µs is shown in Figure 5-(a). This is an average of the distributions after every 10 µs obtained by the post-processing tool. The characteristic mean diameter of D_{90} = 3 µm is computed for the C-1. It has to be noted that this short period of simulation over a relatively

small computational domain is insufficient to predict the final statistics of the aerosol droplet. Nevertheless, it still can be used for the comparison purposes between the cases in this paper.

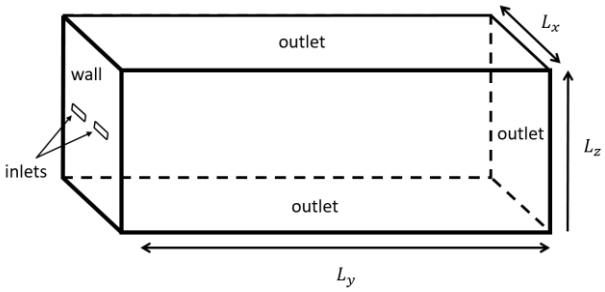

Figure 3. The schematic description of computational domain and boundary conditions.

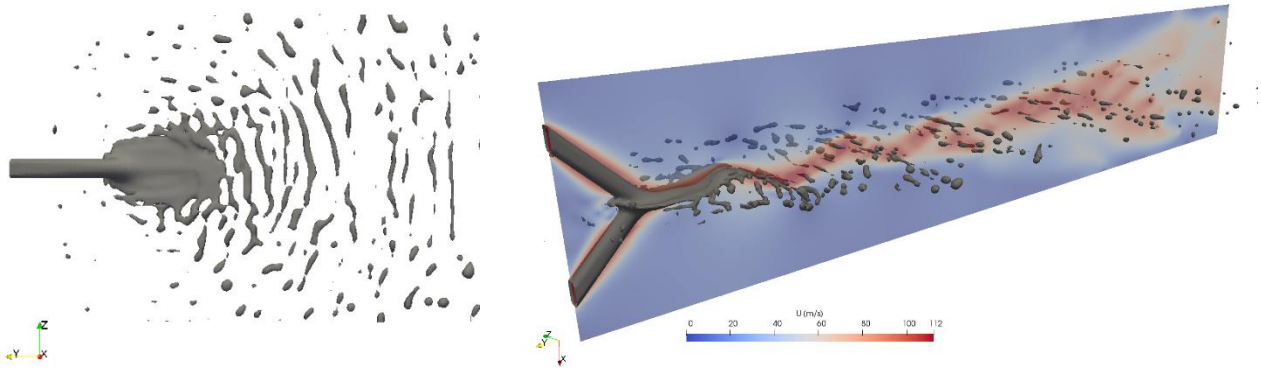

(a) (b)

Figure 4. (a) A top view of the impinged and the disintegration after 100 μs, and (b) one snapshot of the developing atomizing flow with the middle plane velocity contours and iso-contour of α=0.5.

In Figure 4-(b), the oscillatory motion due to the impact waves is evident in the velocity contour downstream the sheet. This harmonic motion has a certain fundamental frequency and is the major player for the atomization. Previous studies such as [11], also explored these harmonic motions to connect the macroscopic flow properties to the atomization. To investigate these harmonics, the velocity fluctuations in the perpendicular direction were recorded every 1e-08 s at the middle of an xz-plane with $10D_h$ distance from the impinging point. The Fast Fourier transform (FFT) analysis of the velocity fluctuation signal for the reference case C-1 is presented in Figure 5-(b). A fundamental frequency of 1.52 MHz and a corresponding velocity amplitude of 4.35 are determined. The variation in operating conditions affects the harmonic characteristics of these waves. As plotted in Figure 6-(a), the 20% variation (increase and decrease) in the velocity of colliding jets results in two different fluctuation spectrum. For the case with lower velocity (C-3), the fundamental frequency decreases drastically. It is the direct consequence of lower kinetic energy and the disappearance of the impact waves. In contrast, the case with higher velocity (C-4) reveals a stronger oscillatory motion with a higher fundamental frequency with larger amplitude. This entails severe instability and results in better atomization. This observation is also supported by Figure 6-(b) which compares the D_{90} and amplitude of fundamental frequency at different velocities.

A similar analysis was performed for the variation of the surface tension. As shown in Figure 7, increasing the surface tension in C-5 has a damping effect on the impact waves and decreases the amplitude of the fluctuation frequencies. On the other hand, decreasing the surface tension (C-6) causes an almost similar fundamental frequency to the C-1, but with a larger amplitude. Besides, a superposition of a second harmonic with higher frequency is notable. This observation is consistent with the consolidating effect of the surface tension in the liquid instability theory. Thus, the impact waves with a lower surface tension are more unstable, and this fact is reflected in the atomization outcome as well. Figure 7-(b) demonstrates that the decrease in surface tension from C-5 to C-6 causes a 6% reduction in the D_{90} of the droplets.

The next parameter to investigate is the collision angle. In the standard SMI device, the collision angle is 90°. In the cases, C-7 and C-8, two different angles of 60° and 120° are studied. The frequency analysis in Figure 8-(a) displays that decreasing the collision angle diminishes the oscillations and a fundamental frequency is barely observed. This

originates from the lower perpendicular component of the velocity of the jets upon impact. On the contrary, the higher collision angle in the case C-8 entails a fundamental frequency with a rather high amplitude.

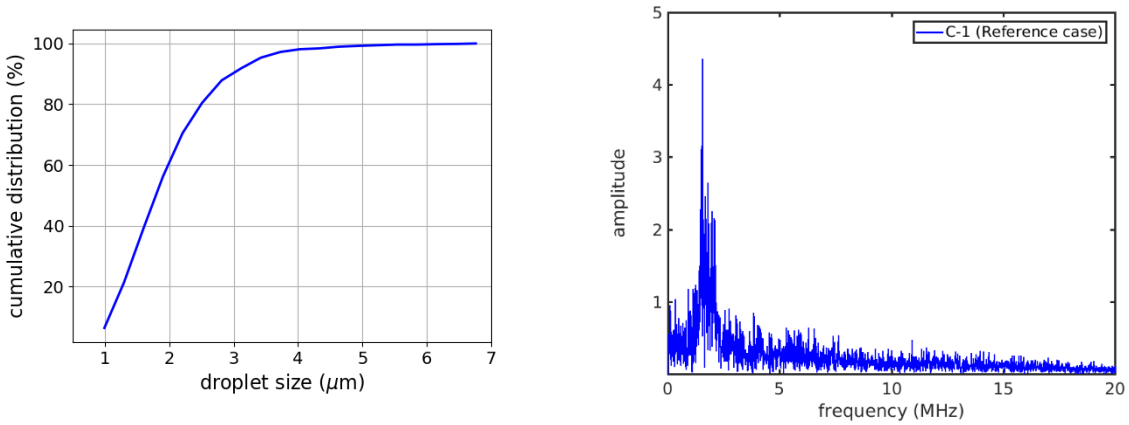

(a) (b)

Figure 5. Reference case: (a) cumulative size distribution of the droplets, and (b) the velocity fluctuation frequency spectrum.

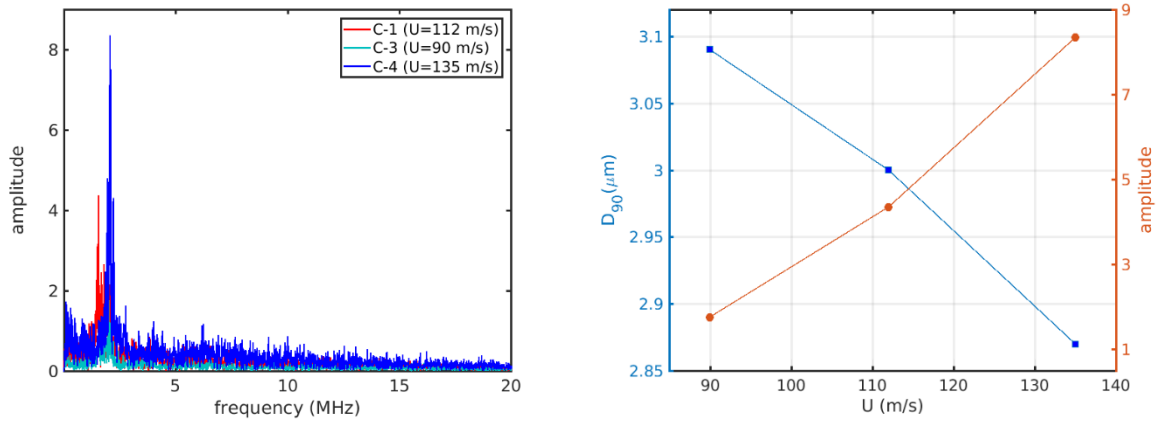

(a) (b)

Figure 6. Variation of colliding jets velocity: (a) the velocity fluctuation frequency spectrum, and (b) spray characteristic size.

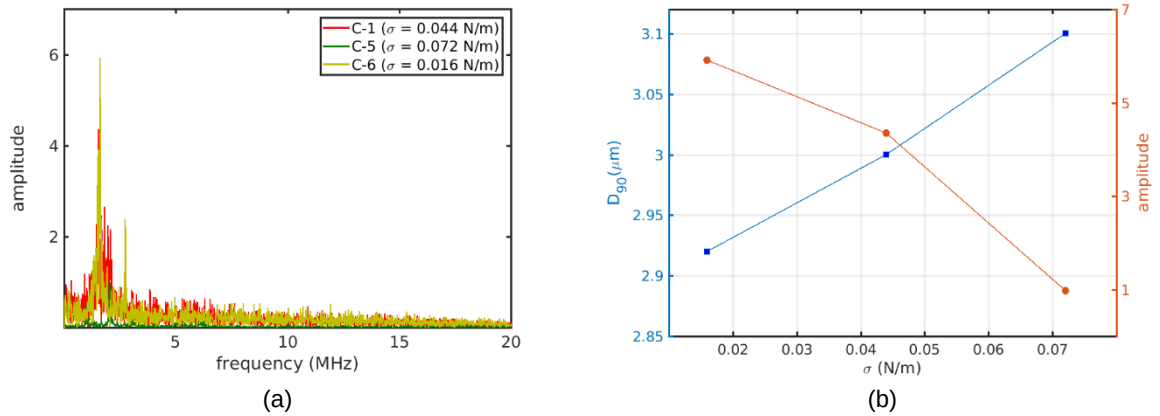

(a) (b)

Figure 7. Variation of surface tension: (a) the velocity fluctuation frequency spectrum, and (b) spray characteristic size.

Nevertheless, an essential phenomenon associated with increasing the collision angle is the backward flow from the impinged sheet region [6]. Because a higher angle causes the impinging point to shift toward the nozzles. To study this backward flow, a plane probe is located in the region between two nozzles to record the liquid flow rate in the backward direction. Figure 8-(b) compares the unsteady liquid mass flux across this plane for the cases C-7 and C-8 compared with the C-1. The values are made dimensionless by the incoming mass flux from the jets. It is

evident that the high collision angle of 120° has a backward flow almost as twice as the reference case, while the lower angle of 60° exhibits no backward liquid flow.

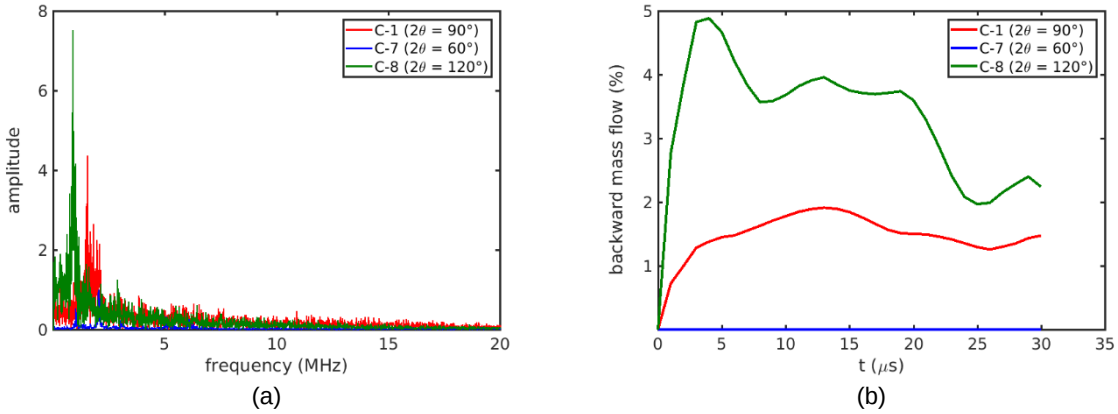

Figure 8. Variation of collision angle: (a) the velocity fluctuation frequency spectrum, and (b) the backward mass flow.

The micro-channels in the SMI device have a rectangular cross-section and emit laminar plain jets. To evaluate the effect of jet shape on the atomization, case C-2 was simulated with two round jets. The velocity fluctuation signals and the size distributions yield no apparent difference with the C-1 at the first glance. But after ensemble averaging of the signal and reducing the background noises, a distinct difference is identified. According to Figure 9-(a), the fundamental frequency in C-1 has a slightly-higher amplitude superposed by a couple of harmonics. Therefore, the plain jets result in more instability and stronger oscillation perpendicular to the sheet. This observation has a direct effect on the orientation of the droplets in downstream. Similar to the backward flow, two plane probes were located close to the front and back patches of the domain in Figure 3 to record the amount of liquid droplets dispersing normal to the sheet direction (i.e. x-direction). This flow rate can serve as an indicator for the perpendicular dispersion of the spray. Figure 9-(b) compares the temporal evolution of this cross flow (normalized by the inlet mass flux) for C-1 and C-2 during the whole simulation time. The spray developed from the plain jet appears to result in a greater perpendicular dispersion of the droplets due to the higher oscillatory motions.

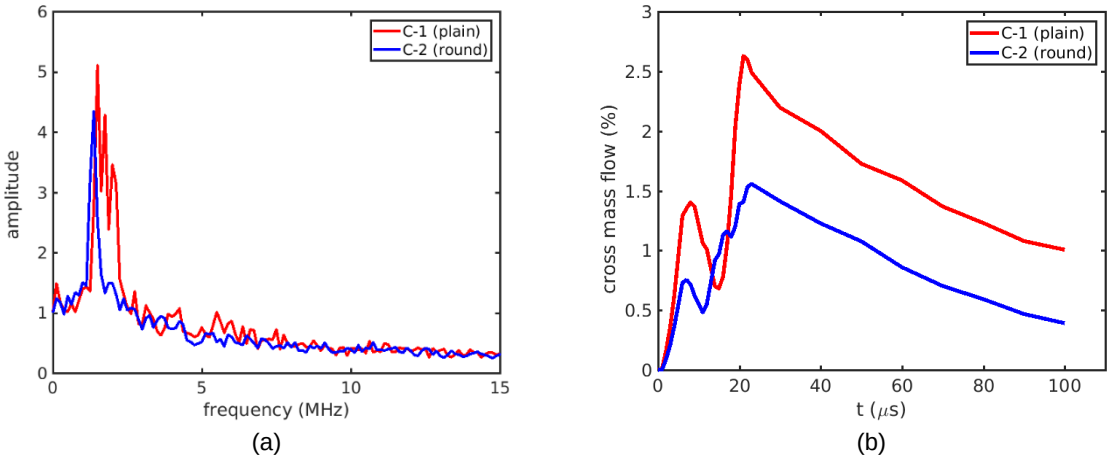

Figure 9. Variation of jet cross-section shape: (a) the ensemble-averaged frequency spectrum, and (b) the unsteady cross flow.

Conclusions

In this paper, a computational study on the colliding atomization of two microfluidic jets in a soft mist inhaler device is performed. According to the operation condition, the micro liquid jets collide and form a sheet which disintegrates into the droplets within the impact wave regime. These unstable waves are the major players for atomization. Using a recently-developed geometrical VOF based on OpenFOAM, the interfacial flow obtained by the liquid jets collision, from the sheet formation towards the downstream atomizing flow, is simulated. Furthermore, the harmonic characteristics of the impact waves were analysed. The droplet size distribution is computed by a post-processing tool. By variation of the design parameters such as the jets velocity, shape, and collision angle as well as the drug solution surface tension, different cases were studied. The simulation results demonstrate that increasing the

injection velocities as well as decreasing the surface tension increases the instability of impact waves and the sheet lateral motion which enhances the atomization. Also, the collision angle is found proportional to the backward liquid flow from the sheet region. In addition, the jets cross-section shape appears to control the circumferential distribution of the generated droplets. This work is the first systematic study on the colliding atomization in microfluidics and provides a connection between the impact wave characteristics and the atomization outcome at different operating conditions. This approach can also be used for the investigation of other types of medical sprays. Nevertheless, a number of shortcomings have to be addressed in future works. Given the fact that the interactions between surface tension and the unsteady motions of the impact wave control the colliding atomization, an improved two-phase LES formulation such as [23], with proper subgrid models for surface tension and interface dynamics may improve the accuracy of the investigation. Also, the post-processing of the spray properties has to be improved by longer simulation time and larger computational domain with grid independence study. To this end, the adaptive mesh refinement functionality of the isoAdvector approach will be used to optimize the computational cost for each case.

Acknowledgments
The author acknowledges the financial support from STRATEC Consumables GmbH in Austria.

Nomenclature

α	volume of fluid [-]
t	time [s]
ρ	density [kg m^{-3}]
μ	dynamic viscosity [kg m^{-1} s^{-1}]
σ	surface tension [kg s^{-2}]
U	velocity [m s^{-1}]
p	pressure [kg m^{-1} s^{-2}]
D	rate of deformation [s^{-1}]
Re	Reynolds number [-]
We	Weber number [-]
δ_s	Dirac delta function [-]
$\hat{n}$	interface normal vector [-]
κ	interface curvature [m^{-1}]
f	frequency [s^{-1}]
D_{90}	characteristic droplet size [m]
D_h	hydraulic diameter [m]

References

[1] Martin A. R. and Finlay W. H., 2015, Expert Opinion on Drug Delivery, 12, pp. 889-900.
[2] Dietzel, A., 2016, “Microsystems for pharmatechnology: Manipulation of fluids, particles, droplets, and cells.”
[3] Ahsgriz, N., 2011, “Handbook of Atomization and Sprays: Theory and Applications.”
[4] Wachtel, H., Kattenbeck, S., Dunne, S., Disse, B., 2017, Pulmonary Therapy, 3, pp. 19-30.
[5] Dombrowski, N., and Hooper, P. C., 1963, Journal of Fluid Mechanics, 18, pp. 392-400.
[6] Ibrahim A. E. and Przekwas A. J., 1991, Physics of Fluids A: Fluid Dynamics, 3, 2981.
[7] Ryan, H. M., Anderson, W. E., Pal, S., Santoro, R. J., 1995, Journal of Propulsion and Power, 11, pp. 135-145.
[8] Bremond, N. and Villermaux, E., 2006, Journal of Fluid Mechanics, 549, pp. 273-306.
[9] Li, R. and Ashgriz, N., 2006, Physics of Fluids, 18, 087104.
[10] Chen, X., Ma, D., Yang, V. and Popinet, S., 2013, Atomization and sprays, 23, pp. 1079-1101.
[11] Zhang, P.Y. and Wang, B., 2017, Physics of Fluids, 29 (4), pp. 392-400.
[12] Bush, J. W. M. and Hash, A. E., 2004, Journal of Fluid Mechanics, 511, pp. 285-310.
[13] Chen, X. and Yang, V., 2019, Chinese Journal of Aeronautics, 32, pp. 45-57.
[14] Hirt, C. and Nichols, B., 1981, Journal of Computational Physics, 39, pp. 201-225.
[15] Ruan, C., Xing, F., Huang, Y., Xu, L., Lu, X., 2017, Atomization and sprays, 27 (12), pp. 1025-1040.
[16] Popinet, S., 2003, Journal of Computational Physics, 190, pp. 572-600.
[17] Weller, H., Tabor, G., Jasak, H., Fureby, C., 1998, Computers in Physics, 12, pp. 620-631.
[18] Dolatkhahi, H., Oliaee, G., Kebriaee, A., Sep. 6.-8. 2017, 28th European Conference on Liquid Atomization and Spray Systems.
[19] Roenby, J., Bredmose, H., Jasak, H., 2016, Royal society open science, 3, 160405.
[20] Longest, P. W. and Hindle, M., 2009, Journal of Aerosol Medicine and Pulmonary Drug Delivery, 22 (2), pp. 99-112.
[21] Brackbill, J., Kothe, D., Zemach, C., 1992, Journal of Computational Physics, 100, pp. 335-354.
[22] Vallier, A., Revstedt, J., Nilsson, H., Oct. 6.-8. 2011, 4th International Meeting on Cavitation and Dynamic Problems in Hydraulic Machinery and Systems.
[23] Saeedipour, M., Vincent, S., Pirker, S., 2019, International Journal of Multiphase Flow, 112, pp. 286-299.